Energy Proceedings
Vol 53, 2025
ISSN 2004-2965

Sub-rib microstructural flow channel design for application in water electrolysis#

Haokai Xu[1 2], Jian Huang[1 2], Kaijie Luo[1 2], Penglin Yang[1 2], Dingding Ye[1 2], Liang Zhang[1 2], Jun Li[1 2*], Xun Zhu[1 2], Qiang Liao[1 2]
1 Key Laboratory of Low-grade Energy Utilization Technologies and Systems, Chongqing University, Ministry of Education, Chongqing, 400044, China
2 Institute of Engineering Thermophysics, School of Energy and Power Engineering, Chongqing University, Chongqing, 400044, China
(Corresponding Author: lijun@cqu.edu.cn)

ABSTRACT

The flow channel structure relates to the flow channel and PTL contact resistance and mass transfer performance in the channel, especially at larger operating voltage, the gas transfer and ohmic loss seriously affect the Proton Exchange Membrane water electrolysis performance. In this paper, the flow channel sub-rib microstructure is designed, and the effects of different sub-rib microstructure designs on the performance of the electrolysis are compared by means of experiments and simulations, and the distributions of micro-vertebrae under the rib of the flow channel and liquid water in the channel, ohmic losses and mass transfer efficiency are analyzed to obtain the optimal design of the flow channel microstructure. The experimental results show that the 0.03 mm tabs under the rib can effectively reduce the interfacial ohmic resistance and improve the mass transfer, and the experimental performance is improved by 9.98% relative to the conventional flow channel, while the simulation results in a performance improvement of 14.30%.

Keywords: Proton Exchange Membrane water electrolysis, flow channel, sub -rib microstructure, ohmic losses, mass transfer

NONMENCLATURE

Abbreviations	
PEMWE	Proton Exchange Membrane water electrolysis
CD	Current Distributors
CH	Flow Channel
PTL	Porous Transport Layer
CL	Catalyst Layer
MEM	Membrane

1. INTRODUCTION

Renewable energy sources, such as solar and wind, have gained widespread attention with the growing concern for energy efficiency and environmental sustainability, however, the volatility and intermittency of renewable energy sources are the main challenges for their practical applications. In order to effectively utilize the excess energy from intermittent renewable energy sources, PEMWE is a compelling solution for energy storage and green hydrogen production due to its high efficiency, high purity and fast response [1]. However, widespread commercialization of PEMWE faces significant challenges due to expensive precious metal catalysts and complex mass transfer issues under high voltage conditions [2]. Current research has emphasized the advancement of novel catalysts and electrode materials to reduce the cost of PEMWE, and limited attention has been paid to investigating the mass transfer difficulties under high voltage conditions, and it has been reported that high bubble coverage and gas aggregation in the channel will adversely affect the electrolysis performance and durability, making it critical to control the mass transfer [3].

As an important part of PEMWE, the flow channel assumes the role of supplying and distributing the reactants uniformly in the active region, as well as improving the gas discharge of the products. Currently, the most commonly described in the literature make parallel flow channel, single serpentine flow channel and multi-serpentine flow channel, because of the different structural forms and flow channel distribution, all reactants and products in single serpentine flow channel must pass through a flow channel, so the flow rate and pressure drop of single serpentine flow channel are higher [4]. In addition to the design of flow channel distribution, the performance of PEMWE is also affected by the depth of the flow channel, Majasan et al. [5]

This is a paper for the 16th International Conference on Applied Energy (ICAE2024), Sep. 1-5, 2024, Niigata, Japan.

demonstrated that the effect of different flow channel depths on mass transfer has a non-monotonic trend, implying the possibility of optimal design of the flow channel. In addition, there are also studies on the design of the flow channel structure to improve the bubble desorption rate. Wu et al. [6] analyzed the feasibility of the design by designing a double-layer flow channel structure through experiments, and the results showed that the bubbles in the channel could be quickly drawn into the degassing layer, providing more space for the electrode water supply.

Although the bubbles inside the flow channel can be observed experimentally, it must be recognized that the high cost of the experiment and the complexity of observing the two-phase flow state inside the flow channel are attached to the larger limitations, therefore, it is imperative to explore the evolution of the bubbles as well as the two-phase transport characteristics through numerical simulation, and it is easier to predict and propose guidance for designing the flow channel with different optimized structures. Lin et al. [7] constructed three-dimensional three-phase models with three different flow structures, and investigated the internal flow velocity and pressure distributions by constructing three-dimensional model to study the internal flow velocity and pressure distribution, and the simulation and experimental results are consistent, which provides theoretical support for the selection and optimization of electrolytic water flow channel and working conditions. Park et al. [8] analyzed the effects of anode flow channel structure and PTL permeability on the performance by constructing a three-dimensional two-phase flow model, and the results show that the slot rib-width ratio and PTL permeability are also higher, the better the performance.

However, the above simulation studies can seldom be combined with experiments due to their over-idealized working conditions, and the simulation of relatively complex structures is difficult to realize for industrial applications, so the effect of flow channel design on the performance of PEM electrolytic water remains to be explored. Therefore, in this study, an sub-rib microstructure flow channel form was designed, and a three-dimensional two-phase electrochemical model was established to investigate the effect of the sub-rib structure on the ohmic and mass transfer of the electrolytic water, and it was verified by combining experiments and simulations that the structure could effectively improve the sub-rib mass transfer of the flow channel and the overall performance of the electrolysis. The results of this study provide an optimized flow channel design to improve the sub-rib bubble discharge.

2. EXPERIMENTAL AND MODELING

2.1 Sub-rib microstructure

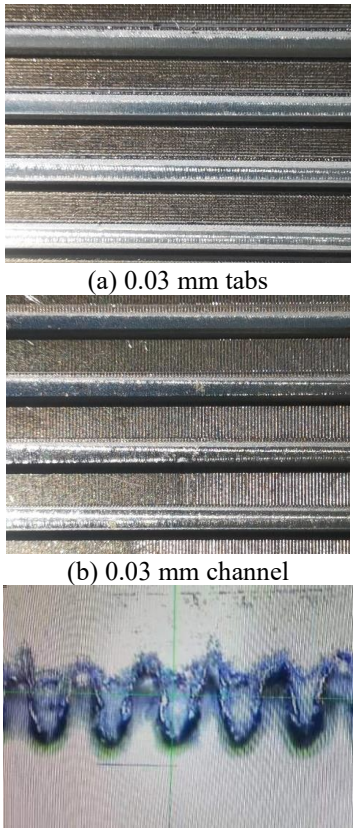

(a) 0.03 mm tabs

(b) 0.03 mm channel

(c) Side view of 0.03mm tab

Fig. 1 Localized enlargement of subcostal microstructure

In this study, a conventional serpentine flow channel structure was fabricated with a channel width and rib width of 1 mm, followed by femtosecond laser machining for microstructural machining under the rib of the flow channel, with the microstructural form divided into micro-tabs and channels, and the width of the tops of the tabs and channels was 0.03 mm, as shown in Fig. 1 Localized sub-rib microstructures. To ensure the effect of surface roughness due to laser processing, the Ti flow channel plate was washed with ethanol in an ultrasonic bath for 30 min after processing.

2.2 PEMWE fabrication

In this study, the membrane electrode assembly was made of catalyst cladding membrane (CCM) of Nafion 115 membrane with an effective area of 4.84 cm^2 (2.2 cm × 2.2 cm), in which the anode was IrO_2 with a loading of 0.5 mg/cm^2 and the cathode was Pt/C catalyst with a loading of 0.2 mg/cm^2. Both the anode and cathode were

made of titanium felts with a thickness of 0.25 mm as a porous transport layer (PTL), and 0.2 mm PTFE gaskets were used to prevent water leakage. The cell cathode and anode are clamped by stainless steel end plates and have four evenly spaced bolts.

2.3 PEMWE Model

In this study, Fluent was used to construct the single-flow channel structure as shown in Fig. 2, the PEMWE assembly size and catalyst loading were fabricated based on the experiments, and a two-phase electrochemical model was constructed to investigate PEMWE based on the multinomial mixing model, which is capable of describing the gas-liquid flow in the porous medium driven by the capillary pressure, and the controlling equations and the source terms used in this study are given in Table 1 [9].

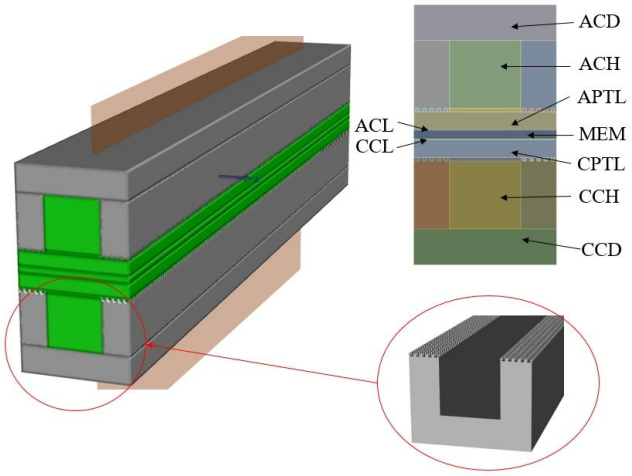

Fig. 2 PEM electrolyzed water single channel model and local structure

The electrochemical control equations in this paper are based on the B-V equation:

$$V_{act} = \frac{RT}{\alpha_{an}F}\sin h^{-1}(\frac{i}{2i_{0,an}}) + \frac{RT}{\alpha_{ca}F}\sin h^{-1}(\frac{i}{2i_{0,ca}}) \quad (1)$$

where α is the charge transfer coefficient, and the exchange current density i_0 makes the current normalized by the geometric effective area of the PEM water electrolysis.

$$i_0 = i_{0,ref}\ \exp(-\frac{E_A}{R}(\frac{1}{T}-\frac{1}{T_{ref}})) \quad (2)$$

The ohmic overpotential is caused by the ohmic resistance R of different parts of the PEM water electrolysis:

$$V_{ohm} = RI = (R_{fp} + R_{\lg dl} + R_{ccm})I \quad (3)$$

Concentration overpotentials are caused by limitations in the supply of reactants or by the blockage of active catalyst sites by excess products:

$$V_{con} = \frac{RT}{4F}\ln(\frac{c_{O_2,me}}{c_{O_2,me,0}}) + \frac{RT}{2F}\ln(\frac{c_{H_2,me}}{c_{H_2,me,0}}) \quad (4)$$

The open circuit voltage depends on the available voltage and the activity of reactants and products and can be expressed by the Nernst equation as follows:

$$E_0 = 1.23 + \frac{RT}{2F}\ln(\frac{p_{H_2}p_{O_2}^{0.5}}{p_{H_2O}}) \quad (5)$$

Table 1 Governing equations and source terms of the PEMWE model.

	Governing equations	*Source terms*
Mass	$\nabla\bullet(\rho u) = S_m$	$S_m = S_{H_2O}M_{H_2O} + S_{H_2}M_{H_2} + S_{O_2}M_{O_2}$
Momentum	$\nabla\bullet(\rho uu) = -\nabla p + \nabla\bullet\tau + S_u$	$S_u = -\frac{\mu}{K}u$
Water	$\nabla\bullet(\gamma_c u c_{H_2O}) = \nabla\bullet[(\frac{c^g_{H_2O}}{\rho^g} - \frac{c^l_{H_2O}}{\rho^l})J_l] + S_{H_2O}$	$S^{an}_{H_2O} = -\frac{j}{2F} - \frac{n_d j}{F}$
Hydrogen	$\nabla\bullet(\gamma_c u c_{H_2}) = \nabla\bullet(\frac{D^{H_2}_{g,eff}}{1-s}\nabla c_{H_2}) + \nabla\bullet(\frac{c^g_{H_2}}{\rho^g}J_l) + S_{H_2}$	$S^{ca}_{H_2O} = \frac{j}{2F}$
Oxygen	$\nabla\bullet(\gamma_c u c_{O_2}) = \nabla\bullet(\frac{D^{O_2}_{g,eff}}{1-s}\nabla c_{O_2}) + \nabla\bullet(\frac{c^g_{O_2}}{\rho^2}J_l) + S_{O_2}$	$S^{an}_{O_2} = \frac{j}{4F}$
Electron	$\nabla\bullet(\sigma^s_{eff}\nabla\phi_s) + S_s = 0$	$S^{an}_s = -j$, $S^{ca}_s = j$
Proton	$\nabla\bullet(\sigma^e_{eff}\nabla\phi_e) + S_e = 0$	$S^{an}_e = j$, $S^{ca}_e = -j$

2.4 Boundary conditions

Due to the complexity of the PEMWE transport phenomena, the model is divided into external and internal boundaries, with the fluid region solving for the matter conservation equation, the electron charge conservation equation in all regions except the MEM and the CD, and the ionic charge conservation equation in the ACL, MEM, and CCL regions. The anode inlet is set up as a liquid water mass flow inlet (5. 87 × 10^{-6} kg/s) with an inlet water temperature of 353.15 K, the cathode inlet is a fluid-free inlet (u = 0 m/s), the cathode and anode outlets are constant-pressure outlets at 1 atmosphere, and the CD is surrounded by a constant temperature of 298.15 K.

3. RESULTS AND DISCUSSION

3.1 Experimental performance

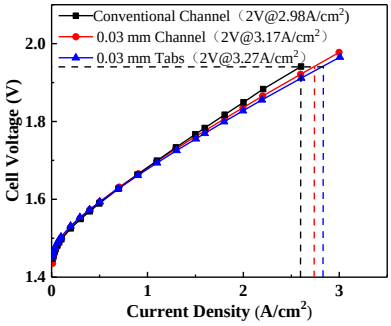

(a) polarization curve

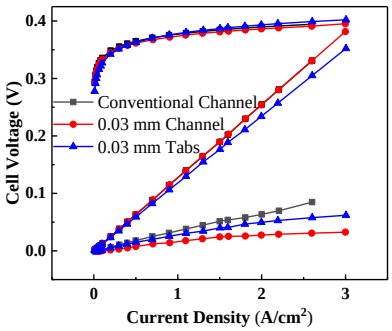

(b) polarization loss

Fig. 3 Performance of different channel structures and polarization partitioning

The same cathodic flow channel plate was used for all experiments, and only the effect of microstructure under the rib on anodic mass transfer and ohmic was investigated. As shown in Fig. 3(a) for the comparison of polarization curves between the conventional flow channel and the one with microstructures, the performance of the optimized flow channel with microstructures under the ribs were all improved compared to the conventional flow channel plate, as shown by the polarization partitioning in Fig. 3(b), the 0.03 mm channel under the rib can effectively improve the mass transfer loss, which is due to the pressure difference between two neighboring channels in the single-serpentine flow channel design, and the sub-rib slot can force the oxygen to be rapidly detached from the rib, to Avoiding the accumulation of excessive oxygen concentration under the rib (PTL) improves the mass transfer performance. At the same time, although the sub-rib channel may reduce some of the flow channel and the contact area of the PTL, its ohmic loss is not improved and is basically the same as that of the conventional flow channel (Fig. 3(b)). The 0.03 mm tabs under the rib not only improves the mass transfer under the rib, but also reduces the ohmic loss, which is due to the tabs structure under the rib is embedded in the PTL, which has micropores of 0.03 to 0.06 mm, and such microstructures have the potential to be embedded in the pores of the PTL to improve the contact surface, which in turn reduces the ohmic. The best performance is achieved by the 0.03 mm tabs sub-rib microstructure in this section of experiments (2 V @ 3.27 A/cm^2), which improves the performance by 9.98% compared to the conventional flow channel.

3.2 Numerical simulation

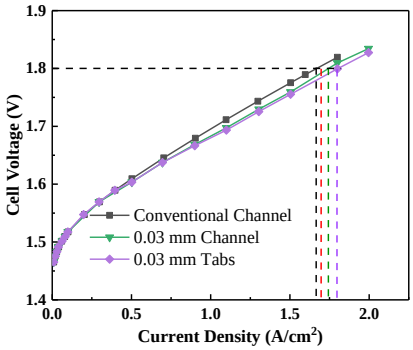

(a) polarization curve

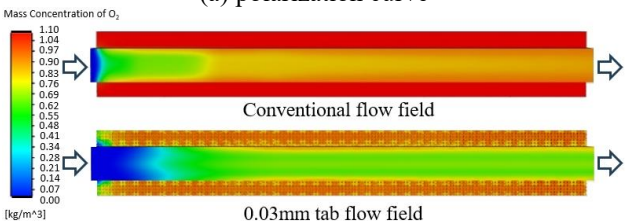

(b) Oxygen mass content map

Fig. 4 Performance of different channel structures and oxygen distribution

By establishing a single-flow channel model of multiphase electrochemical PEM electrolytic water and constructing a flow channel structure with sub-rib microstructure, the conventional flow channel structure was compared and analyzed. The simulated polarization curve results are shown in Fig. 4(a), and the simulation results are consistent with the experimental results. Fig. 4(b) shows the comparison of the oxygen content of the electrolysis at 1.7 V working voltage, it can be seen that the oxygen content under the rib of the conventional flow channel is high, and a large amount of oxygen accumulation leads to high mass transfer loss, while the flow channel with microstructure can effectively alleviate the oxygen accumulation under the rib, and at the same time, the model is constructed as a half-embedded, i.e., the total height of the microstructure is 0.05 mm, and the embedded depth of the PTL is 0.025 mm, which increases the contact between flow channel and PTL, and improves the contact between flow channel

and PTL. The contact between the channel and PTL is improved, and therefore the ohmic loss decreases, which is consistent with Section 3.1. The simulation results show a 14.3% improvement in channel performance for the 0.03 mm tabs compared to the conventional channel.

4. CONCLUSION

In this study, we propose the microstructures of the flow channel sub-rib bosses and slots, and investigate the effects of the sub-rib structures on the mass transfer and performance of the flow channel using experimental and simulation methods. The results show that the single serpentine flow channel sub-rib structure can force the rapid desorption of oxygen under the rib and thus improve the mass transfer efficiency, while the tab structure may be embedded in the PTL to improve the contact surface between the flow channel and the PTL, and the tabs structure not only reduces the ohmic loss, but also effectively improves the sub-rib mass transfer to achieve the best performance. Under the working condition of voltage of 2 V, the experimental results of 0.03 mm tabs were improved by 9.98% and the simulated results were improved by 14.3% compared with the conventional channel. In this study, the overall performance is effectively improved by designing the microstructure, while its processing difficulty is low, which provides a new idea for the optimized design of the flow channel of the subsequent electrolysis.

ACKNOWLEDGEMENT

The authors gratefully acknowledge the financial support from the Projects of INTERNATIONAL COOPERATION and Exchanges NSFC (No. 52261135628), and the Innovative Research Group Project of the National Natural Science Foundation of China (No. 52021004), and the China Postdoctoral Science Foundation (No.2022M710508).

REFERENCE

[1] Majasan J O, Cho J I S, Dedigama I, Tsaoulidis D, Shearing P, Brett D J L. Two-phase flow behaviour and performance of polymer electrolyte membrane electrolysers: Electrochemical and optical characterisation. international journal of hydrogen energy, 2018, 43(33): 15659-15672.

[2] Feng Q, Liu G, Wei B, Wei B, Zhang Z, Li H, et al. A review of proton exchange membrane water electrolysis on degradation mechanisms and mitigation strategies. Journal of Power Sources, 2017, 366: 33-55.

[3] Bazarah A, Majlan E H, Husaini T, Zainoodin A M, Alshami I, Goh J, et al. Factors influencing the performance and durability of polymer electrolyte membrane water electrolyzer: A review. International journal of hydrogen energy, 2022, 47(85): 35976-35989.

[4] Maier M, Smith K, Dodwell J, Hinds G, Shearing P R, Brett D J L. Mass transport in PEM water electrolysers: A review. International Journal of Hydrogen Energy, 2022, 47(1): 30-56.

[5] Majasan J O, Cho J I S, Maier M, Dedigama I, Shearing P R, Brett D J L. Effect of anode flow channel depth on the performance of polymer electrolyte membrane water electrolyser. ECS transactions, 2018, 85(13): 1593.

[6] Wu L, Pan Z, Yuan S, Shi X, Liu Y, Liu F, et al. A dual-layer flow field design capable of enhancing bubble self-pumping and its application in water electrolyzer. Chemical Engineering Journal, 2024, 488: 151000.

[7] Lin R, Lu Y, Xu J, Huo J, Cai X. Investigation on performance of proton exchange membrane electrolyzer with different flow field structures. Applied Energy, 2022, 326: 120011.

[8] Park S, Lee W, Na Y. Performance comparison of proton exchange membrane water electrolysis cell using channel and PTL flow fields through three-dimensional two-phase flow simulation. Membranes, 2022, 12(12): 1260.

[9] Qian X, Kim K, Jung S. Multiphase, multidimensional modeling of proton exchange membrane water electrolyzer. Energy conversion and management, 2022, 268: 116070.